Population synthesis of common-envelope mergers on the giant branches

Marc van der Sluys

University of Alberta, Edmonton

Mike Politano, Ron Taam, Bart Willems

January 11, 2010

Outline

1. Common-envelope mergers
   - Introduction
   - Population-synthesis models
   - Observational counterparts
   - Conclusions and future work

2. GW astronomy with LIGO/Virgo
   - LIGO/Virgo
   - Binary inspirals
   - Markov-chain Monte Carlo
   - Conclusions

Stellar mergers

Occurrence:

- Collisions: $\tau \sim \frac{1}{2}$ day? (Sills et al. 2001)
- Binary mergers: convective envelope: $\sim \tau_{\rm dyn}$; yr – kyr?
- Binary mergers: radiative envelope: $\tau_{\rm th} \longrightarrow \tau_{\rm dyn}$

Physics:

- Rapid, differential rotation
- Enhanced mixing
- Enhanced mass loss
- Angular momentum!

Stellar mergers

Observability:

- Blue stragglers
- Rapid rotation?
- Abundance anomalies?
- Cluster dynamics
- “Weird” binaries

- B[e] stars?
- V 838 Mon?
- IMBHs?
- Hot subdwarfs?

Detailed collisions

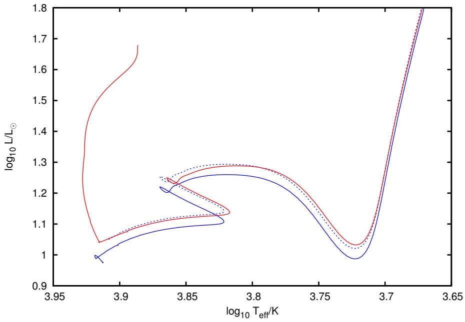

1.75 $M_\odot$: Collision product Normal star

(dashes): Fully mixed model

Glebbeek & Pols, 2008

Use:

- 1D stellar models
- collide them in hydro
- bring remnant in hydrostatic equilibrium
- evolve in 1D
- for low-mass stars: "Entropy" "sorting"

Differences in:

- Timescales
- Luminosities
- Core masses
- Mixing

Input models

Eggleton code TWIN:

- 116 single-star models: 0.5 – 20.0 $M_\odot$ (primary, merger remnant)
- 28 brown-dwarf models: 0.01 – 0.60 $M_\odot$ (secondary)
- Solar composition; X=0.70, Y=0.28, Z=0.02
- Core mass: $M_\mathrm{c} \equiv$ central region where $X < 0.1$
- Envelope binding energy: $E_\mathrm{bind} \equiv \int_{M_\mathrm{c}}^{M_\mathrm{s}} \left(E_\mathrm{int}(m) - \frac{Gm}{r(m)} \right) \mathrm{d}m$
- Convective mixing: $l/H_P = 2.0$
- Overshooting: none for $M < 1.2\,M_\odot$, $\delta_\mathrm{ov} = 0.12$ for $M \geq 1.2\,M_\odot$
- Stellar wind: "Reimers" (1975), De Jager et al. (1988)
- *Helium-flash-avoidance routine*

Treatment of evolution

Stars

- Constant star-formation rate
- Randomly select 10^7 binaries:
  - $M_{\rm p}$: Miller-Scalo IMF
  - $q \equiv M_{\rm s}/M_{\rm p}$: $g(q)\,{\rm d}q = \{1, q, q^{-0.9}\}\,{\rm d}q$
- Follow the evolution of track closest in mass to primary
- When mass comes closer to next track, jump with conservation of $M_{\rm c}$

Orbit

- Assume synchronous rotation on RGB, AGB: $\omega_{\rm p} = \omega_{\rm orb}$
- Mass and AM loss from stellar wind
- If $v_{\rm rot} > v_{\rm crit}$: lose additional mass and AM until $v_{\rm rot} \leq v_{\rm crit}$
- Redistribute AM, so that $J_{\rm tot} = (I_{\rm p} + I_{\rm orb})\,\omega_{\rm orb}$
- $v_{\rm crit} \equiv \{0.1, 1/3, 1.0\}\,v_{\rm br}$

Common envelope and spiral-in

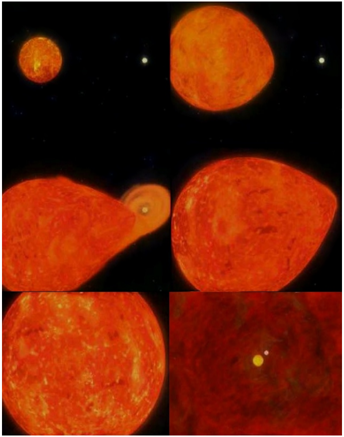

- CE occurs when:
  - $R_\mathrm{p} > R_\mathrm{RL,p}$ and $q > q_\mathrm{crit}(M_\mathrm{p}, M_\mathrm{c})$ (Hurley et al. 2002)
  - $J_\mathrm{prim} > \frac{1}{3} J_\mathrm{orb}$ (Darwin 1879)
- Classical energy formalism to determine post-CE orbit (Webbink 1984):

$$E_\mathrm{bind} = \alpha_\mathrm{CE} \left(\frac{G M_\mathrm{p} M_\mathrm{s}}{2\, a_\mathrm{i}} - \frac{G M_\mathrm{c} M_\mathrm{s}}{2\, a_\mathrm{f}} \right)$$

- $\alpha_\mathrm{CE} = \{0.1, 0.5, 1.0\}$
- Merger occurs if after CE: $R_\mathrm{RL,s} < R_\mathrm{s}$

Merger product

The merged object has:

- the core mass of the original primary
- the maximum mass for which the star is spinning sub-critically (and $M \leq M_{\rm p} + M_{\rm s}$)
- the evolutionary state of the primary, or later

The merged object does:

- evolve in the same way as a single star
- lose additional mass to ensure that $v_{\rm rot} \leq v_{\rm crit}$

Population-synthesis results

	Number	Fraction of previous group	Fraction of initial population
Total binary population:	**10,000,000**	**100%**	**100%**
No MT	7,094,523	71%	71%
Stable MT	1,267,854	13%	13%
Unstable MT:	**1,637,623**	**16%**	**16%**
CE Survivors:	789,807	48%	7.9%
Mergers:	**847,816**	**52%**	**8.5%**
Mergers due to RLOF	689,815	81%	6.9%
Mergers due to tidal capture	158,001	19%	1.6%
Mergers on RGB	738,385	87%	7.4%
Mergers on AGB	109,431	13%	1.1%
WDs	822,773	97%	8.2%
GB/HB stars:	**25,042**	**3%**	**0.25%**
RGB	**9,301**	**37%**	**0.09%**
HB	**14,306**	**57%**	**0.14%**
AGB	**1,435**	**6%**	**0.01%**
Critically rotating RGB stars	297	3.2%	0.003%
Critically rotating HB stars	4,504	31%	0.05%
Critically rotating AGB stars	1	0.1%	0.00001%

Dependence on input parameters

Model	N	$M(M_\odot)$	Fraction with $v_{rot} \leq 0.1\, v_{crit}$	Fraction with $v_{rot} = v_{crit}$	$M_{rej}(M_\odot)$	$\frac{M_{rej}}{M_{bin}}$
standard	25042	1.15	0.0044	0.19	0.65	0.32
$\alpha_{CE} = 0.5$	28271	1.15	0.0050	0.22	0.65	0.32
$\alpha_{CE} = 0.1$	32887	1.10	0.0054	0.27	0.65	0.33
$g(q) = q$	24854	1.15	0.0050	0.20	0.95	0.41
$g(q) = q^{-0.9}$	10528	1.20	0.0044	0.20	0.10	0.08
$v_{crit} = v_{br}$	24415	1.30	0.0054	0.13	0.50	0.25
$v_{crit} = 0.1\, v_{br}$	25491	1.10	0.0058	0.20	0.75	0.35
single stars	294118	1.20	0.997	0.0	...	...

Politano et al., in preparation

Merger properties

Total mass:

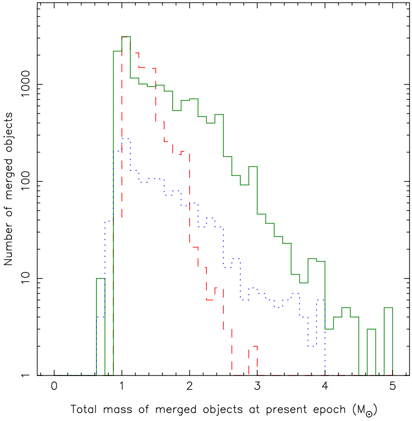

Luminosity:

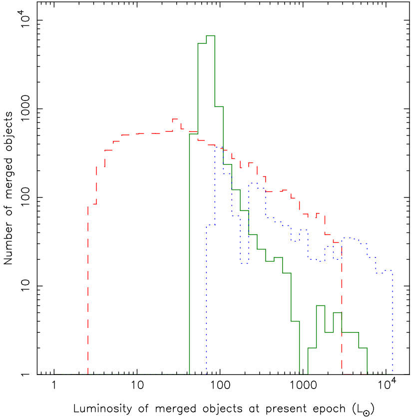

RGB **HB** **AGB**

$v_{\rm crit} = \frac{1}{3} v_{\rm br}$

Politano et al., in preparation

Merger population

All merged objects:

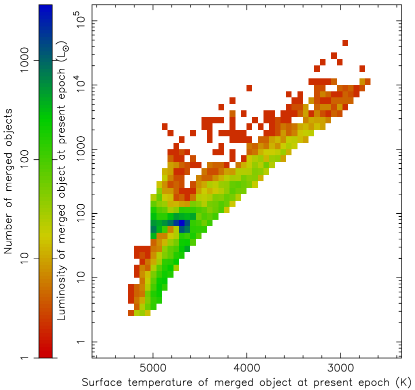

Merged objects on HB:

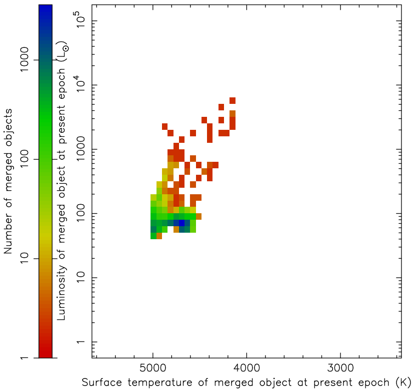

$v_{\rm crit} = \frac{1}{3} v_{\rm br}$

Politano et al., in preparation

Rotational velocities

v_{rot}/v_{crit}:

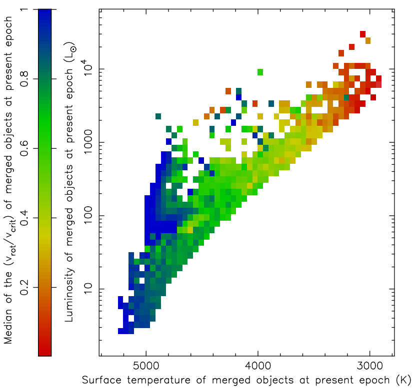

v_{rot} sin i (km/s):

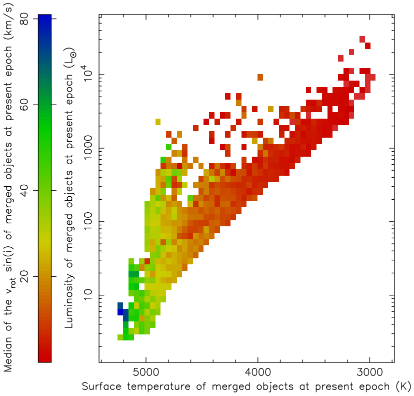

$$v_{crit} = \frac{1}{3} v_{br}$$

Politano et al., in preparation

Rotational velocities

Single stars:

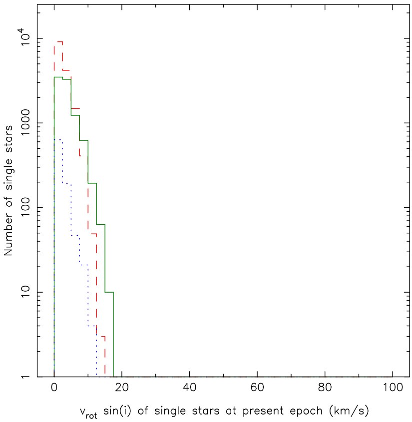

Merger remnants:

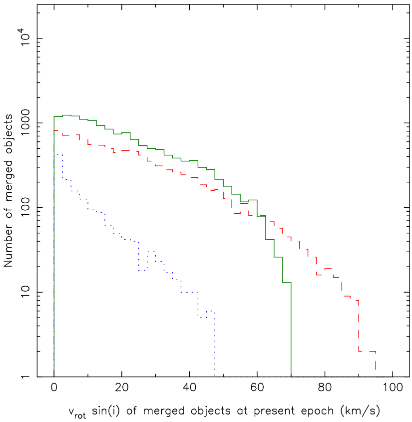

RGB **HB** **AGB**

$v_{crit} = \frac{1}{3} v_{br}$

Politano et al., in preparation

sdB stars

Basic properties:

- Core helium burning stars with very thin ($\lesssim 0.02\,M_\odot$) hydrogen-rich envelope
- In the field $\sim$ 40–70% are found in binaries
- In GCs mostly observed as **single** sdB stars
- Masses observed $\sim 0.39\,M_\odot$ – $0.7\,M_\odot$ (*e.g.* asteroseismology)

sdB stars

Possible formation channels:

In wide binaries:

- One or two phases of stable Roche-lobe overflow

In close binaries:

- One or two CE/spiral-in phases

Single sdB stars:

- He-WD–He-WD mergers ($M \gtrsim 0.4\,M_\odot$)
- Strong mass loss at tip of RGB (*e.g.* capture of planet; Soker & Harpaz, 2000, 2007; Livio & Siess, 1999a,b)
- **CE merger on the RGB** (Soker 1998, Soker & Harpaz 2000, 2007)

Rotational velocities for merged HB stars

All merged objects:

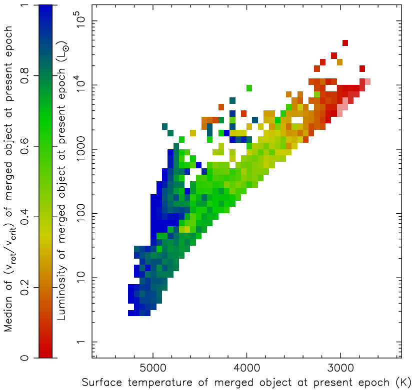

Merged objects on HB:

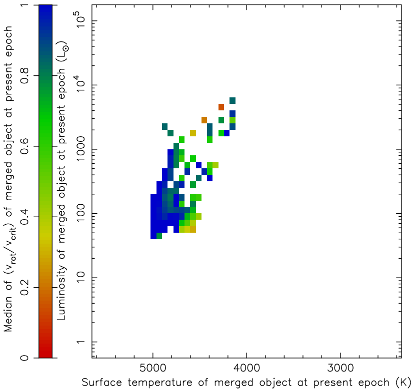

$$v_{crit} = \frac{1}{3} v_{br}$$

Politano et al., in preparation

Rotational velocities

v_{rot}/v_{crit}:

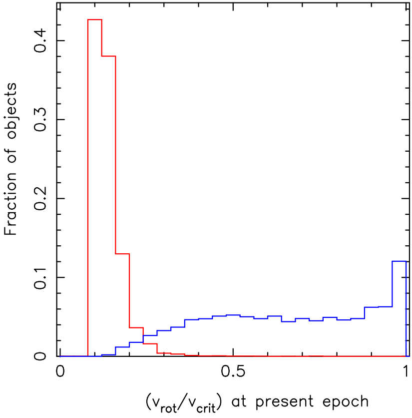

v_{rot}(km/s):

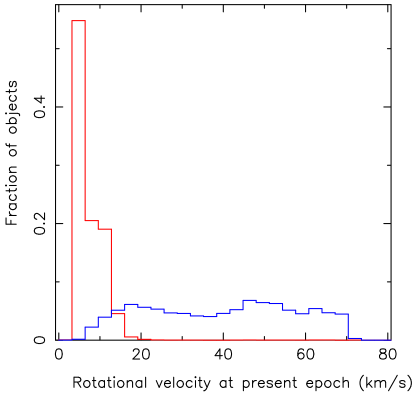

Merged objects **Single stars**

$v_{crit} = \frac{1}{3} v_{br}$

Politano et al., in preparation

Core and envelope masses

Helium-core masses:

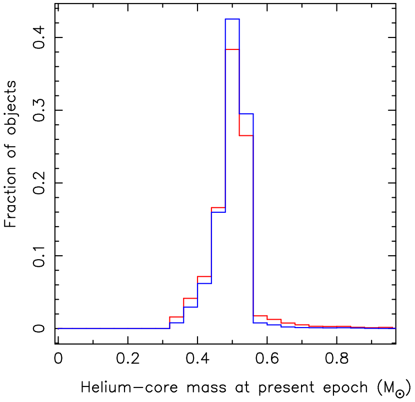

Envelope masses:

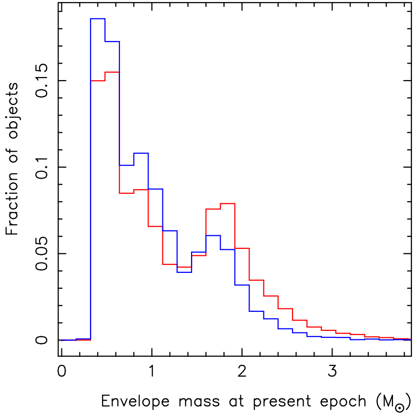

Merged objects **Single stars**

Losing the envelope

Detailed model of an HB star with initial parameters M $\approx$ 0.59 $M_\odot$, $M_{env} \approx 0.11\,M_\odot$ and $v_{rot} \approx 25$ km/s:

M_{env} vs. $\log R$:

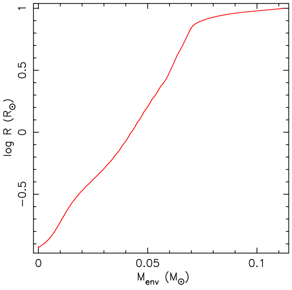

M_{env} vs. T_{eff}:

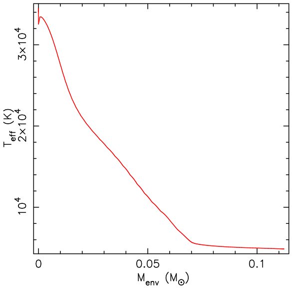

M_{env} vs. v_{rot}:

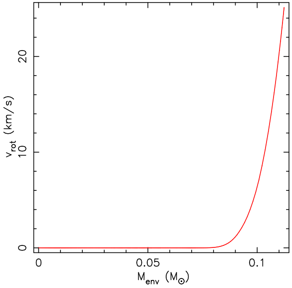

Lithium-rich giants

Reddy & Lambert 2005; Kumar & Reddy 2009:

Star	[Fe/H]	T_{eff}	$M_\star/M_\odot$	$\log L/L_\odot$	$\log \epsilon$(Li)	$^{12}C/^{13}C$
HD 77361	−0.02 ± 0.1	4580 ± 75	1.5 ± 0.2	1.66 ± 0.1	3.82 ± 0.10	4.3 ± 0.5
HD 233517	−0.37	4475 ± 70	1.7 ± 0.2	2.0[a]	4.22 ± 0.11	...
IRAS 13539−4153	−0.13	4300 ± 100	0.8 ± 0.7	1.60[a]	4.05 ± 0.15	20
HD 9746	−0.06	4400 ± 100	1.92 ± 0.3	2.02	3.75 ± 0.16	28 ± 4
HD 19745	−0.05	4700 ± 100	2.2 ± 0.6	1.90[a]	3.70 ± 0.30	16 ± 2
IRAS 13313−5838	−0.09	4540 ± 150	1.1	1.85[a]	3.3 ± 0.20	12 ± 2

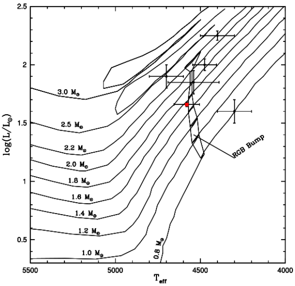

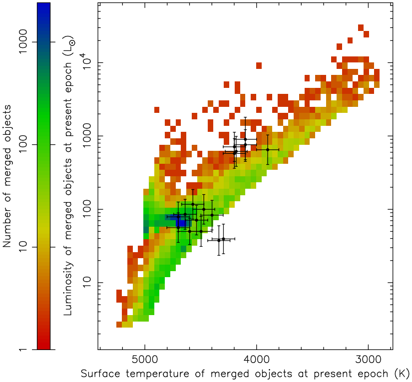

Oblateness

Zhao et al. 2009

α Cep

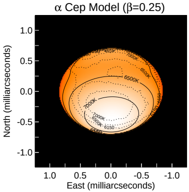

$e = 0.60$

α Oph

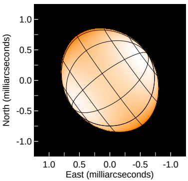

$e = 0.55$

$$e \equiv \sqrt{1 - \left(R_{\rm pol}/R_{\rm eq}\right)^2}$$

MacLaurin (1742) spheroids:

$$\frac{\omega}{\sqrt{2\pi G\rho}} = \sqrt{\frac{\sqrt{1-e^2}}{e^3}\left(e - 2e^2\right)\,\mathrm{asin}(e) - \frac{3}{e^2}\left(1-e^2\right)}$$

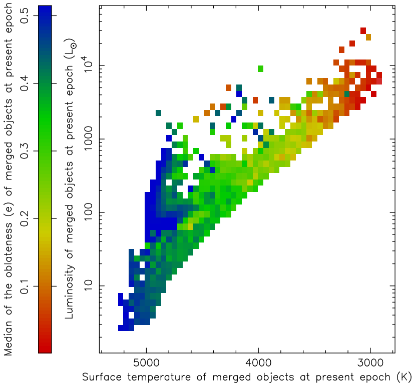

Oblateness

Single stars

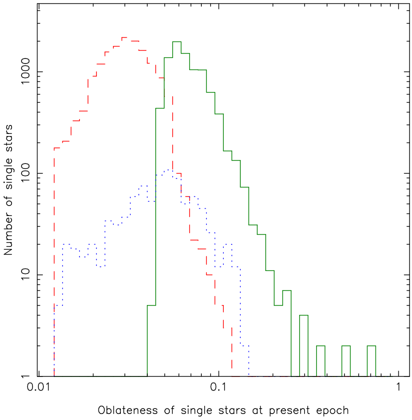

Merger products

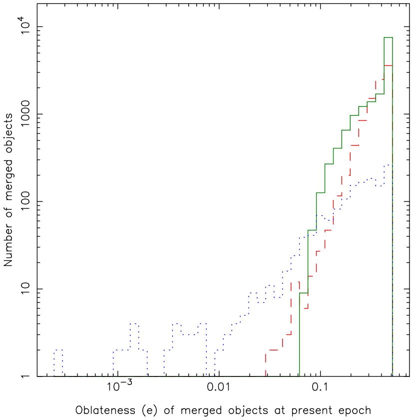

Politano et al., in preparation

Asymmetric planetary nebulae?

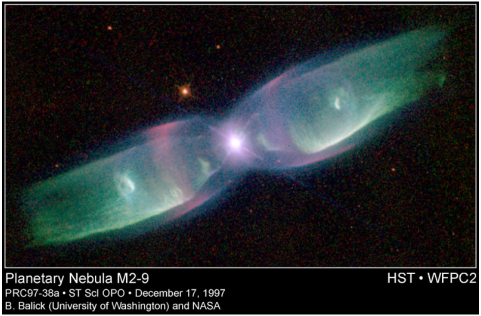

Butterfly nebula (HST)

Conclusions

Population-synthesis code:

- We produced an initial version of a code with which we can study large populations of merger remnants, albeit with simplified methods
- We find that common-envelope mergers on the giant branches lead to rapidly rotating merger products
- Indirect telltales of (former) rapid rotation may include abundance anomalies, small envelope mass, oblate stars, IR excess and asymmetric nebulae

sdB stars:

- Contraction of a merged object due to helium ignition provides a natural way to create rapidly rotating HB stars
- A small fraction of these HB stars have thin envelopes; these stars are close to becoming single sdB stars

Future work

- Use more flexible implementation for mass loss due to winds and rotation
- Include magnetic braking for merged object
- Look for mechanism to remove last bit of HB-star envelope (perhaps on RGB?)
- Combine population synthesis and “entropy” “sorting”:
  - do population synthesis to get the mergers
  - use entropy sorting to get a merged object
  - interpolate to create an evolution model
  - evolve it with a detailed stellar-evolution code (including rotation)

And now for something completely different...

Gravitational-wave astronomy with LIGO/Virgo: the SPINSPIRAL code

Marc van der Sluys

University of Alberta, Edmonton

Vivien Raymond, Ilya Mandel, Vicky Kalogera

January 11, 2010

Outline

Laser Interferometer GW Observatory (LIGO)

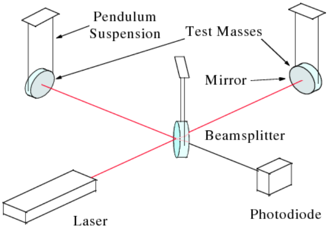

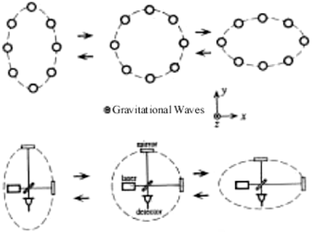

Predicted detection rates

Realistic estimate:

	Rates (yr^{-1})			Horizon (Mpc)		
	NS-NS	BH-NS	BH-BH	NS-NS	BH-NS	BH-BH
Initial	0.015	0.004	0.01	32	67	160
Enhanced	0.15	0.04	0.11	71	149	349
Advanced	20	5.7	16	364	767	1850

Plausible, optimistic estimate:

	Rates (yr^{-1})			Horizon (Mpc)		
	NS-NS	BH-NS	BH-BH	NS-NS	BH-NS	BH-BH
Initial	0.15	0.13	1.7	32	67	160
Enhanced	1.5	1.4	18	71	149	349
Advanced	200	190	2700	364	767	1850

Estimates assume $M_{\rm NS} = 1.4\,M_\odot$ and $M_{\rm BH} = 10\,M_\odot$

CBC group, rates document

Goals for SPINSPIRAL

LIGO

- Show that Markov-Chain Monte Carlo (MCMC) with a large number of parameters (12–15) on LIGO data can be done
- Automated parameter estimation on detected inspiral signal:
  - Confirm spinning inspiral nature of signal
  - Determine *physical* parameters (masses, spin, position, . . .)

Astrophysics

- BH/NS mass distributions, BH spins and spin alignments
- Merger rates, NS-NS/BH-NS/BH-BH merger ratios
- Gravity in strong regime; NS EoS
- Association of GW and EM events, *e.g.* GRB
- Evolution of massive stars (in binaries), CEs
- Initial-mass range for BH progenitors

Inspiral waveforms with increasing spin

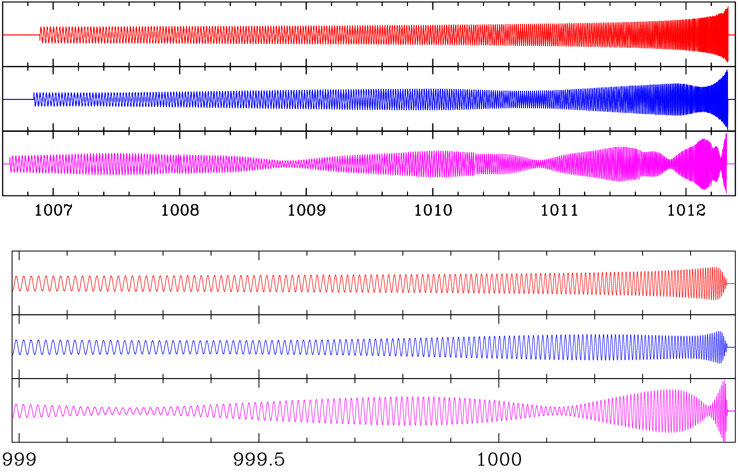

$a_{\mathrm{spin}} \equiv S/M^2 = 0.0$, 0.1 and 0.5

Signal injection into detector noise

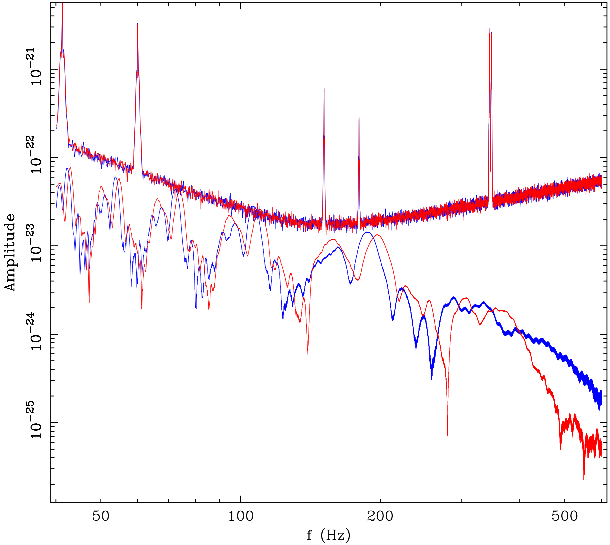

- Using 2 4-km detectors H1, L1
- Gaussian, stationary noise
- Do 1.5-pN software injections
- Retrieve physical parameters with 1.5-pN template

Here, ΣSNR = 17

Compute posterior distribution

- Find posterior density of the model parameters
- Bayesian approach
- The likelihood for each detector *i* is:

$$L_i(d|\vec{\lambda}) \propto \exp\left(-2\int_0^\infty \frac{\left|\tilde{d}(f) - \tilde{m}(\vec{\lambda}, f)\right|^2}{S_n(f)}\,\mathrm{d}f\right)$$

- Coherent network of detectors:
  - $\mathrm{PDF}(\vec{\lambda}) \propto \mathrm{prior}(\vec{\lambda}) \times \prod_i L_i(d|\vec{\lambda})$

- Use Markov-Chain Monte Carlo to sample the posterior

Markov chains

- Choose starting point for chain: $\vec{\lambda}_1$
- Compute its likelihood: $L_j \equiv L(d|\vec{\lambda}_j)$ and prior: $p_j \equiv p(\vec{\lambda}_j)$
- do $j = 1, N$
  - draw random jump size $\Delta\vec{\lambda}_j$ from Gaussian with width $\vec{\sigma}$
  - consider new state $\vec{\lambda}_{j+1} = \vec{\lambda}_j + \Delta\vec{\lambda}_j$
  - calculate $L_{j+1} \equiv L(d|\vec{\lambda}_{j+1})$ and $p_{j+1} \equiv p(\vec{\lambda}_{j+1})$
  - if($\frac{p_{j+1}}{p_j} \frac{L_{j+1}}{L_j} >$ ran_unif[0,1]) then
    - Accept new state $\vec{\lambda}_{j+1}$
    - Increase jump size $\vec{\sigma}$
  - else
    - Reject new state; $\vec{\lambda}_{j+1} = \vec{\lambda}_j$
    - Decrease jump size $\vec{\sigma}$
  - end if
  - save state $\vec{\lambda}_{j+1}$
- end do (j)

SPINSPIRAL example

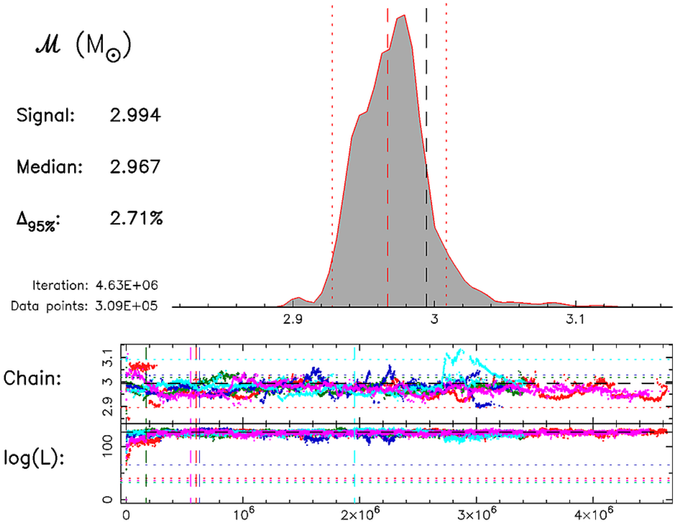

MCMC analyses

MCMC parameters

Masses: $\mathcal{M} \equiv (M_1 + M_2)\,\eta^{3/5}$ & $\eta \equiv \frac{M_1 M_2}{(M_1+M_2)^2}$, distance: $\log d_L$, time and phase at coalescence: t_c & φ_c, position: R.A. & sin Dec, spin magnitude: $a_{\mathrm{spin}_{1,2}}$, spin orientation: $\cos\theta_{\mathrm{spin}_{1,2}}$ & $\varphi_{\mathrm{spin}_{1,2}}$, orientation: $\cos(\iota)$ & ψ

MCMC set-up

- 5 serial chains per run, starting from the true parameter values
- Chain length: 5×10^6 states, burn-in: 5×10^5 states
- Run time: 10 days on a 2.8 GHz CPU for 1.5-pN waveform ($\sim 2.5\times$ longer for 3.5-pN)

- Signals injected in simulated noise for H1L1V @ SNR $\approx$17.0
- Fiducial binary: $M_{1,2} = 10 + 1.4\,M_\odot$, $d_L = 16$–21 Mpc
- Spin: $a_{\mathrm{spin}} = 0.0, 0.1, 0.5, 0.8$, $\theta_{\mathrm{SL}} = 20^\circ, 55^\circ$

MCMC results for inspirals with spin

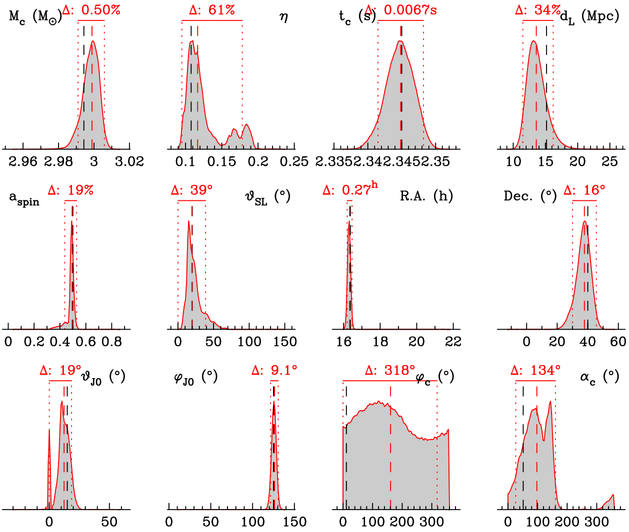

Parameters:

- H1 & L1
- $M = 10, 1.4\,M_\odot$
- $d_L = 18.7\,\mathrm{Mpc}$
- $a_{\rm spin} = 0.5$, $\theta_{\rm SL} = 20^\circ$
- $\Sigma\mathrm{SNR} \approx 17.0$
- Black dashed line: true value
- Red dashed line: median
- Δ's: 90% probability

MCMC results for inspirals with spin

Spinning BH, non-spinning NS:

$10 + 1.4\,M_\odot$, 16–22 Mpc, Σ SNR=17

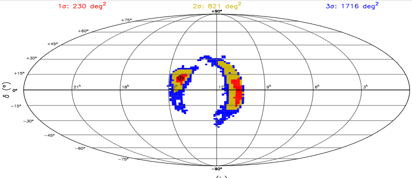

2 detectors, $a_{\rm spin} = 0.0$

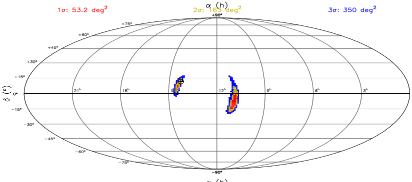

2 detectors, $a_{\rm spin} = 0.5$

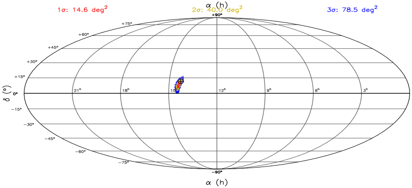

3 detectors, $a_{\rm spin} = 0.5$

van der Sluys et al., 2008; Raymond et al., 2009

Accuracy of parameter estimation

2 detectors (H1 & V):

$a_{\rm spin}$	$\theta_{\rm SL}$ (°)	$d_{\rm L}$ (Mpc)	M_1 (%)	M_2 (%)	$\mathcal{M}$ (%)	η (%)	t_c (ms)	$d_{\rm L}$ (%)	$a_{\rm spin}$	$\theta_{\rm SL}$ (°)	**Pos.** (°^{2})	**Ori.** (°^{2})
0.0	0	16.0	95	83	2.6	138	18	86	0.63	—	537	19095
0.1	20	16.4	102	85	1.2	90	10	91	0.91	169	406	16653
0.1	55	16.7	51	38	0.88	59	7.9	58	0.32	115	212	3749
0.5	20	17.4	53[b]	42[a]	0.90	50[b]	5.4	46[a]	0.26	56	111[a]	3467[a]
0.5	55	17.3	31	24	0.62	41	4.9	21	0.12	24	19.8	178[a]
0.8	20	17.9	54[a]	42[a]	0.86[a]	54[a]	6.0	56	0.16	25[a]	104[a]	1540
0.8	55	17.9	21	16	0.66	29	4.7	22	0.15	15	22.8	182[a]

3 detectors (H1, L1 & V):

$a_{\rm spin}$	$\theta_{\rm SL}$ (°)	$d_{\rm L}$ (Mpc)	M_1 (%)	M_2 (%)	$\mathcal{M}$ (%)	η (%)	t_c (ms)	$d_{\rm L}$ (%)	$a_{\rm spin}$	$\theta_{\rm SL}$ (°)	**Pos.** (°^{2})	**Ori.** (°^{2})
0.0	0	20.5	114	90	2.6	119	15	69	0.98[b]	—	116	4827
0.1	20	21.1	70	57	0.92	72	7.0	60	0.49	160	64.7	3917
0.1	55	21.4	62	48	0.93	68	6.2	51	0.52	123	48.7	976
0.5	20	22.3	54[b]	44[a]	0.89[a]	48[b]	3.3	52	0.28[a]	69	28.8	849
0.5	55	22.0	33	25	0.62	43	4.6	23[a]	0.14	27	20.7	234[a]
0.8	20	23.0	53[b]	41[a]	0.85[a]	52[b]	3.8	55	0.17	23[a]	36.4[a]	645
0.8	55	22.4	30	22	0.86	40	5.0	26	0.21	21	27.2	288

90%-probability ranges, injection SNR = 17.0
[a] the true value lies outside the 90%-probability range
[b] idem, outside the 99%-probability range, but inside the 100% range

van der Sluys et al., 2008

Analysis of a signal with two spins

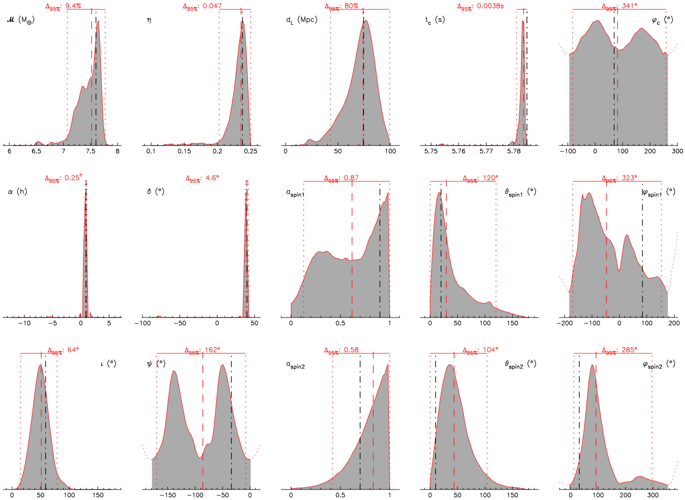

- 3.5-pN waveform
- 3 detectors (H1,L1,V)
- $\mathcal{M} = 7.6\,M_\odot$, $\eta = 0.238$; $M_1 = 11.0\,M_\odot$, $M_2 = 7.0\,M_\odot$
- $a_{\rm spin} = 0.9, 0.7$
- $d_{\rm L} = 74.5\,{\rm Mpc}$
- Σ SNR=15

van der Sluys et al., in preparation

Analysis of a signal with two spins

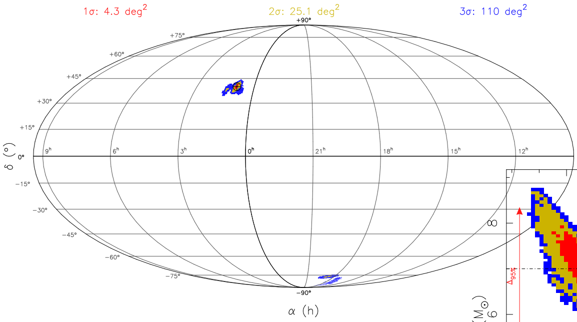

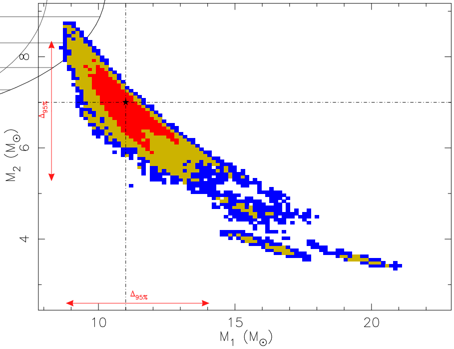

van der Sluys et al., in preparation

Non-spinning analysis of a signal with spin

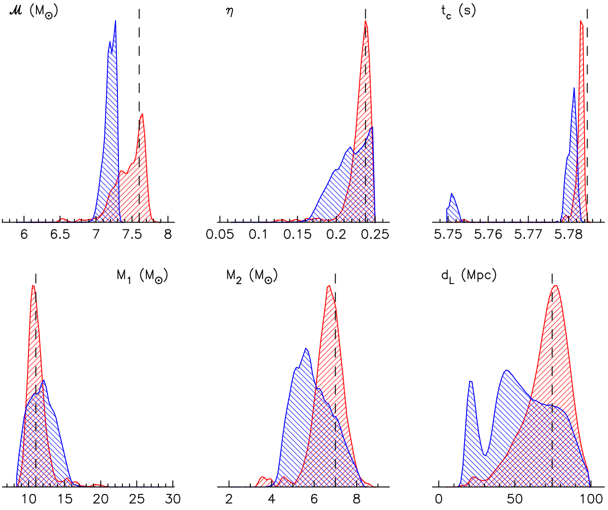

Signal with spins

Recovery with spinning template

Recovery with non-spinning template

van der Sluys et al., in preparation

Conclusions GW parameter estimation

GW parameter estimation code:

We have developed the code SPINSPIRAL which can recover the 12–15 parameters of a binary inspiral, including one or two spins, using a Markov-chain Monte-Carlo technique

Accuracies for analysis with 2 detectors:

- For a detection with only 2 detectors, the presence of spin increases the accuracy of parameter estimation
- In this case, we can produce astronomically relevant information, with typical accuracies for lower / higher spin:
  - individual masses: $\sim$ 32% / 39%
  - dimensionless spin: $\sim$ 0.60 / 0.18
  - distance: $\sim$ 55% / 45%
  - sky position: $\sim$ 500°^2} / 40°^2}
  - binary orientation: $\sim$ 2500°^2} / 175°^2}
  - time of coalescence: $\sim$ 11 ms / 6 ms

Conclusions GW parameter estimation

Accuracies for analysis with 3 detectors:

- The addition of a third detector increases SNR and hence the accuracy for parameter estimation in general
- Because of the extra timing information, the accuracy of the sky position, and as a result, of the binary orientation gain disproportionally
- For a detection with 3 detectors, the position of the source is restricted to two or one well-defined patch(es) in the sky
- These accuracies can lead to association with an electromagnetic detection (*e.g.* gamma-ray burst)

Inclusion of spin in parameter estimation:

- The inclusion of spin adds a significant number of dimensions and introduces (strong) correlations
- Failing to take into account spin can result to biases in especially mass parameters

End...